THE JOURNAL OF BIOLOGICAL CHEMISTRY VOL. 286, NO. 43, pp. 37304–37312, October 28, 2011

The *Azoarcus* Group I Intron Ribozyme Misfolds and Is Accelerated for Refolding by ATP-dependent RNA Chaperone Proteins*[S]

Received for publication, July 29, 2011, and in revised form, August 26, 2011 Published, JBC Papers in Press, August 30, 2011, DOI 10.1074/jbc.M111.287706

Selma Sinan[‡§1], **Xiaoyan Yuan**[‡], **and Rick Russell**[‡2]

From the [‡]*Department of Chemistry and Biochemistry, Institute for Cellular and Molecular Biology, University of Texas at Austin, Austin, Texas 78712 and the* [§]*Balıkesır University, Science and Art Faculty, Department of Biology, Molecular Biology, Balıkesır 10000, Turkey*

Background: Group I introns are valuable for studying RNA folding and chaperone proteins.
Results: A catalytic activity assay was developed and used to demonstrate two prominent phases for *Azoarcus* ribozyme folding. The slow phase displays hallmarks of a misfolded intermediate.
Conclusion: This RNA accumulates a misfolded intermediate and interacts productively with RNA chaperones.
Significance: Delineating misfolding and chaperone roles is crucial for understanding how cellular RNAs fold.

Structured RNAs traverse complex energy landscapes that include valleys representing misfolded intermediates. In *Neurospora crassa* and *Saccharomyces cerevisiae*, efficient splicing of mitochondrial group I and II introns requires the DEAD box proteins CYT-19 and Mss116p, respectively, which promote folding transitions and function as general RNA chaperones. To test the generality of RNA misfolding and the activities of DEAD box proteins *in vitro*, here we measure native folding of a small group I intron ribozyme from the bacterium *Azoarcus* by monitoring its catalytic activity. To develop this assay, we first measure cleavage of an oligonucleotide substrate by the prefolded ribozyme. Substrate cleavage is rate-limited by binding and is readily reversible, with an internal equilibrium near unity, such that the amount of product observed is less than the amount of native ribozyme. We use this assay to show that approximately half of the ribozyme folds readily to the native state, whereas the other half forms an intermediate that transitions slowly to the native state. This folding transition is accelerated by urea and increased temperature and slowed by increased Mg^{2+} concentration, suggesting that the intermediate is misfolded and must undergo transient unfolding during refolding to the native state. CYT-19 and Mss116p accelerate refolding in an ATP-dependent manner, presumably by disrupting structure in the intermediate. These results highlight the tendency of RNAs to misfold, underscore the roles of CYT-19 and Mss116p as general RNA chaperones, and identify a refolding transition for further dissection of the roles of DEAD box proteins in RNA folding.

Structured RNAs participate in diverse cellular processes, from protein synthesis and regulation to the maintenance of chromosome ends. To achieve their functional structures, RNAs traverse complex folding landscapes that typically include multiple intermediates and alternative structures. Indeed, nearly every RNA that has been studied *in vitro* has been shown to populate alternative, misfolded structures at equilibrium and/or as kinetic intermediates during folding (1–3). *In vivo*, nearly all processes that involve structured RNAs also require ATP-dependent RNA helicases, the largest group of which is the DEAD box proteins (4). These proteins are proposed to use ATP binding and hydrolysis to disrupt RNA structures, thereby accelerating folding transitions and conformational changes (5–7).

Group I and II introns have been particularly valuable for studies of RNA folding. These RNAs include multiple domains that fold locally and assemble into structures that catalyze excision of the intron from the precursor RNA. They are apparently prone to misfolding *in vivo*, because the DEAD box proteins CYT-19 and Mss116p are required for efficient folding and splicing of multiple introns in the mitochondria of *Neurospora crassa* and *Saccharomyces cerevisiae*, respectively (8, 9). The relative simplicity and tractability of intron RNAs have facilitated detailed studies of RNA folding and RNA chaperone activity by DEAD box proteins (3, 5).

In particular, the folding of group I introns and their ribozyme derivatives has been dissected using biophysical and biochemical approaches (2, 3, 10). When folding is initiated by the addition of Mg^{2+}, RNAs fold from extended conformations that possess secondary structure but lack defined tertiary structure to give compact, highly ordered structures. A ribozyme derived from the *Tetrahymena thermophila* group I intron was shown by chemical footprinting and small angle x-ray scattering (SAXS)[3] to fold through a series of intermediates, becoming compact and structured on time scales ranging from millisec-

* This work was supported, in whole or in part, by National Institutes of Health Grant GM70456 (to R. R.). This work was also supported by Welch Foundation Grant F-1563 (to R. R.).
[S] The on-line version of this article (available at http://www.jbc.org) contains supplemental Table S1 and Figs. S1–S3.
[1] Supported by a fellowship from the Scientific and Technological Research Council of Turkey.
[2] To whom correspondence should be addressed: Dept. of Chemistry and Biochemistry, 1 University Station A4800, University of Texas at Austin, Austin, TX 78712. Tel.: 512-471-1514; Fax: 512-232-3432; E-mail: rick_russell@mail.utexas.edu.

[3] The abbreviations used are: SAXS, small angle x-ray scattering; MOPS, 3-(*N*-morpholino)-propanesulfonic acid.

onds to minutes (11–15). Further, catalytic activity was used as a probe for native structure formation and revealed that, under commonly used conditions, most of the ribozyme population misfolds on this time scale to a conformation that includes extensive native structure and therefore is not easily distinguished by physical probes (16–18). This misfolded RNA then refolds to the native state more slowly still, in several hours under standard conditions, in a process that involves extensive disruption of native structure (17, 19).

Group I introns have also been used to probe the mechanisms of DEAD box proteins as general RNA chaperones. Early studies showed that CYT-19 promotes a conformational transition in a mutant of the *Tetrahymena* ribozyme (8), and later work showed that CYT-19 accelerates folding transitions of the ribozyme, including refolding of the long-lived misfolded conformation to the native state, by disrupting structure without specifically recognizing misfolded structure (20, 21). This nonspecific activity nevertheless gives accumulation of the native state because it is more stable and unfolded by CYT-19 less efficiently (21, 22). This basic mechanism has been suggested to underlie much of the general RNA chaperone activity by DEAD box proteins (5, 23, 24), but DEAD box protein-assisted folding has been studied for only a relatively small number of RNAs (24–33), and gaps in our understanding of the intrinsic folding processes for some of these RNAs limit the mechanistic insights into the roles of DEAD box proteins.

A second group I intron that has been studied extensively is from a tRNA gene in the bacterium *Azoarcus*. The *Azoarcus* intron is particularly interesting because it has a relatively simple architecture with minimal peripheral structure (see Fig. 1), yet it forms the canonical group I intron core structure with high stability and carries out self-splicing efficiently (34, 35). SAXS and footprinting studies indicated that this RNA acquires structure considerably faster than the *Tetrahymena* ribozyme, with fewer detectable intermediates. Indeed, in early studies the ribozyme appeared to fold to completion in milliseconds (36, 37), although further work has indicated transient formation of intermediates for at least a fraction of the population (38–40).

Here we develop and use a catalytic activity assay to study the folding kinetics of the *Azoarcus* ribozyme, complementing work using physical approaches. We find that approximately half of the population folds readily to the native state, whereas the other half misfolds. Refolding to the native state is on the time scale of an hour at 25 °C and is accelerated by the DEAD box proteins CYT-19 and Mss116p. This RNA and its misfolded conformation should be useful in efforts to understand how RNAs misfold and how DEAD box proteins function as RNA chaperones.

EXPERIMENTAL PROCEDURES

Preparation of RNA—The L-3 *Azoarcus* ribozyme was transcribed *in vitro* from a plasmid that includes a promoter for T7 RNA polymerase immediately upstream from the coding sequence and an EarI restriction site adjacent to the 3′ terminus. The plasmid was digested to completion with EarI, and *in vitro* transcription was performed as described (41). The RNA transcript was purified using a Qiagen RNeasy column as described (16). Substrate and product oligonucleotides were from Dharmacon. RNA concentrations were determined by absorbance at 260 nm using calculated extinction coefficients of $1.95 \times 10^6\ \text{M}^{-1}\ \text{cm}^{-1}$ for the ribozyme, $8.35 \times 10^4\ \text{M}^{-1}\ \text{cm}^{-1}$ for the substrate (CAUACGGCC), $2.96 \times 10^4\ \text{M}^{-1}\ \text{cm}^{-1}$ for the 5′ product, and $6.44 \times 10^4\ \text{M}^{-1}\ \text{cm}^{-1}$ for the 3′ product. The substrate was 5′-end-labeled with [γ-^{32}P]ATP by T4 polynucleotide kinase (New England Biolabs) (41).

Protein Expression and Purification—CYT-19 and Mss116p were expressed as fusion proteins with a cleavable maltose-binding protein and purified as described (23, 27, 42). After purification, proteins were dialyzed against storage buffer (20 mM Tris-Cl, pH 7.5, 500 mM KCl, 1 mM EDTA, 0.2 mM DTT, 50% glycerol), divided into aliquots, flash frozen, and stored at −80 °C.

Protein concentrations were determined by the Bradford assay (Bio-Rad) using bovine serum albumin as a standard. The values were in good agreement with absorbance measurements at 280 nm using extinction coefficients calculated from the amino acid sequences (data not shown).

General Kinetics Methods—For experiments measuring substrate cleavage and ligation, the ribozyme was prefolded at 37 °C (50 mM Na-MOPS, pH 7.0, 10 mM $MgCl_2$, 100 μM guanosine). Cleavage reactions were then initiated at 25 °C by adding 2-fold excess substrate over the ribozyme, including trace ^{32}P-labeled substrate. For reactions with prebound substrate (supplemental Fig. S1*C*), the prefolding step included the substrate but not guanosine, and the incubation was 60 min to ensure complete binding. Guanosine was then added at 25 °C to initiate the cleavage reaction.

Reaction time points (2 μl) were quenched by adding two volumes of 90% formamide, 100 mM EDTA solution with 0.01% (w/v) bromphenol blue, and 0.01% (w/v) xylene cyanol. Radiolabeled substrate and product were separated by 20% polyacrylamide, 7 M urea gel electrophoresis; quantitated by using a phosphorimaging device; and analyzed by ImageQuant (GE Healthcare). The results are presented as the averages and standard errors of at least two independent determinations.

Continuous Catalytic Activity Assay—To initiate the folding and substrate cleavage reactions simultaneously, the ribozyme was added to a solution that included substrate and Mg^{2+}. Final concentrations were 0.4 μM ribozyme, 0.8 μM substrate including trace ^{32}P-labeled substrate, and 10 mM Mg^{2+} (50 mM Na-MOPS, pH 7.0, 100 μM guanosine, 25 °C). Portions of the reaction (2 μl) were withdrawn at various times and quenched and processed as described above.

Discontinuous Catalytic Activity Assay—Folding reactions were performed essentially as described (18). Solution conditions for stage 1 (folding) were 50 mM Na-MOPS, pH 7.0, 10 mM $MgCl_2$, and 1.6 μM ribozyme at 25 °C unless otherwise indicated. At various times, portions of the reaction were added to stage 2 to measure the fraction of native ribozyme by catalytic activity. The conditions for stage 2 were 50 mM Na-MOPS, pH 7.0, 50 mM $MgCl_2$, and 100 μM guanosine at 25 °C. Under these conditions, substrate cleavage is nearly 100-fold faster than the slow phase of folding (see Figs. 2*B* and 6*C*), allowing the cleavage reaction to give a "snapshot" of the fraction of native ribozyme at the time of transfer to stage 2. Control experiments showed that using 10-fold higher guanosine concentration (1

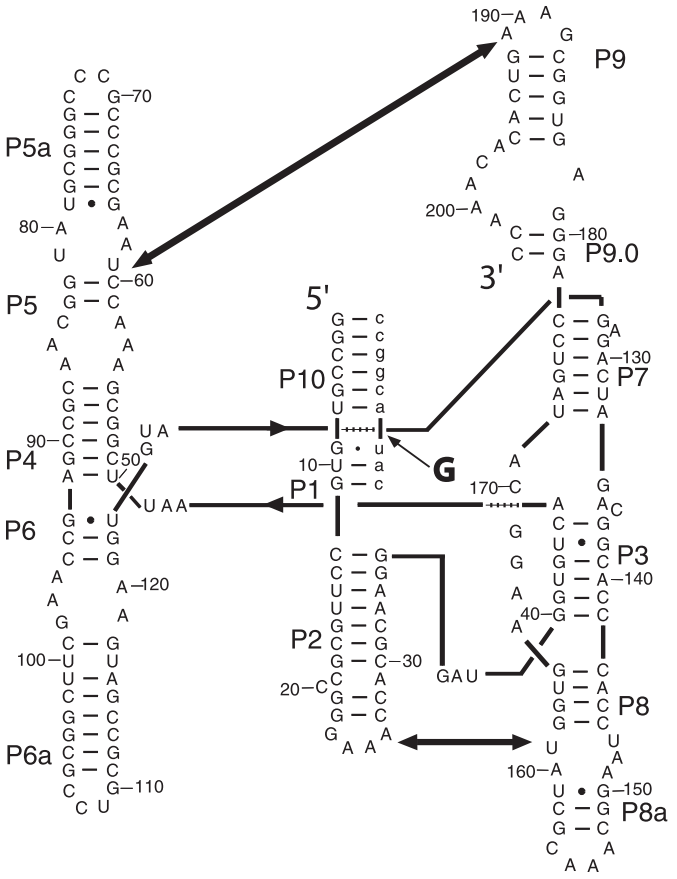

FIGURE 1. **Azoarcus ribozyme construct.** All of the experiments herein used the L-3 ribozyme construct and its 9-nucleotide substrate, as shown (35). Within the ribozyme-substrate complex, paired regions P1 to P10 are labeled, and two canonical tetraloop-receptor tertiary interactions are indicated by *arrows* between the loop L2 and helix P8 and between L9 and P5. The oligonucleotide substrate is shown in *lowercase letters*, and the site of cleavage is indicated by an *arrow* from a *G*, representing the guanosine nucleophile.

mM) gave modestly larger bursts at all folding times, as expected from the results in Fig. 3, but did not affect the measured rate constants for native state formation (data not shown). For reactions with CYT-19 or Mss116p, the protein was destroyed prior to the measurement of catalytic activity by the inclusion of proteinase K (1 mg/ml) in stage 2.

For all of the reactions, the substrate was added in 2-fold excess (0.8 μM substrate, 0.4 μM ribozyme). In early experiments, complete time courses were collected to determine the rate constant and amplitude of the rapid phase of substrate cleavage. In later experiments, a single time point was taken at 15 min. This time is sufficient to allow completion of the rapid phase while minimizing the contribution from the slower phase, which reflects further accumulation of native ribozyme and multiple catalytic turnovers. Time points were quenched and processed as above.

RESULTS

Development of a Catalytic Activity Assay for Folding—To use catalytic activity to follow *Azoarcus* ribozyme folding quantitatively, it was necessary to determine the catalytic properties of the prefolded ribozyme (18). Lacking exons, the ribozyme binds and cleaves a 9-nucleotide substrate that mimics the 5′ splice site (Fig. 1). We sought to identify conditions under

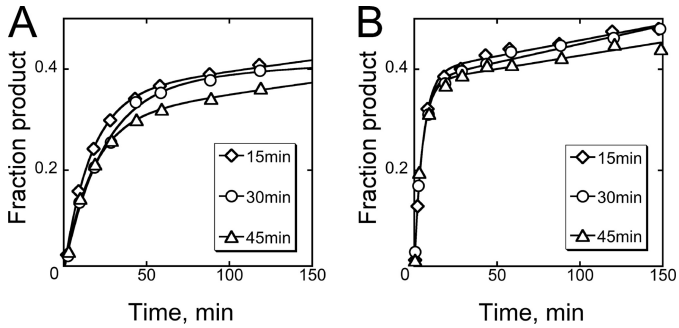

FIGURE 2. **Prefolding of the *Azoarcus* ribozyme.** *A*, the ribozyme (0.4 μM) was folded at 37 °C and 10 mM Mg^{2+} for 15, 30, or 45 min, and then substrate (0.8 μM) was added at 25 °C and 10 mM Mg^{2+}. The plot shows the time course of substrate cleavage monitored by the appearance of product. Multiple independent determinations gave average rate constants of 0.08 min^{-1} and amplitudes of 0.26, with no systematic dependence of either parameter on preincubation time. *B*, substrate cleavage reaction at 25 °C and 50 mM Mg^{2+} after prefolding ribozyme as in *A*. Multiple determinations gave average rate constants of 0.29 min^{-1} and amplitudes of 0.30, again with no systematic dependence on preincubation time. To calculate the ratio of product to ribozyme (see "Results"), the amplitudes were multiplied by two to account for the 2-fold excess of substrate over the ribozyme.

which substrate cleavage is rapid and could therefore reflect the progress of folding. Further, we sought to understand how the burst amplitude in a substrate cleavage reaction, *i.e.* the amount of substrate cleaved rapidly before slow product release limits subsequent turnovers, relates to the amount of native ribozyme. As a starting point, we prefolded the ribozyme with 10 mM Mg^{2+} for various times at 37 °C (15–45 min) and then initiated reactions at 25 °C by adding a 2-fold excess of the substrate. A fraction of the substrate was cleaved in minutes, with a rate constant of 0.08 ± 0.03 min^{-1} (Fig. 2*A*), in a reaction that was rate-limited by substrate binding (supplemental Fig. S1).[4] The progress curves did not depend on preincubation time across the range tested, suggesting that ribozyme folding is complete within 15 min at 37 °C.

Based on previous results with other group I and II introns, we also tested higher Mg^{2+} concentration with the idea that it could increase the rate of the reaction without also increasing the rate of folding and would therefore be useful in folding experiments. Indeed, reactions at 50 mM Mg^{2+}, again after prefolding at 37 °C and 10 mM Mg^{2+}, gave an observed rate constant for cleavage of 0.29 ± 0.05 min^{-1} (Fig. 2*B*), ~4-fold larger than that at 10 mM Mg^{2+}. Therefore, we used 50 mM Mg^{2+} for substrate cleavage in most subsequent experiments.

The burst of cleaved substrate corresponded to 52 ± 4% of the ribozyme population at 10 mM Mg^{2+} and 60 ± 2% at 50 mM Mg^{2+} after accounting for the 2-fold excess of substrate (Fig. 2). The ratio of product to ribozyme did not depend on the ribozyme and substrate concentrations (supplemental Fig. S1),

[4] We found that the rate constant for this burst of substrate cleavage increased linearly with substrate concentration. The dependence of the rate constant on concentration gave a $(k_{cat}/K_M)^S$ value of 6.5 × 10^4 M^{-1} min^{-1} (supplemental Fig. S1*A*), similar to a value determined previously for reactions at 20 °C and 15 mM Mg^{2+} (57), and this rate constant was confirmed by single turnover measurements across a wider range of ribozyme concentrations (supplemental Fig. S1*B*). The rate-limiting step under these conditions is substrate binding, because reactions in which substrate was preincubated with the ribozyme and then substrate cleavage was initiated by guanosine addition gave substantially larger rate constants (supplemental Fig. S1*C*).

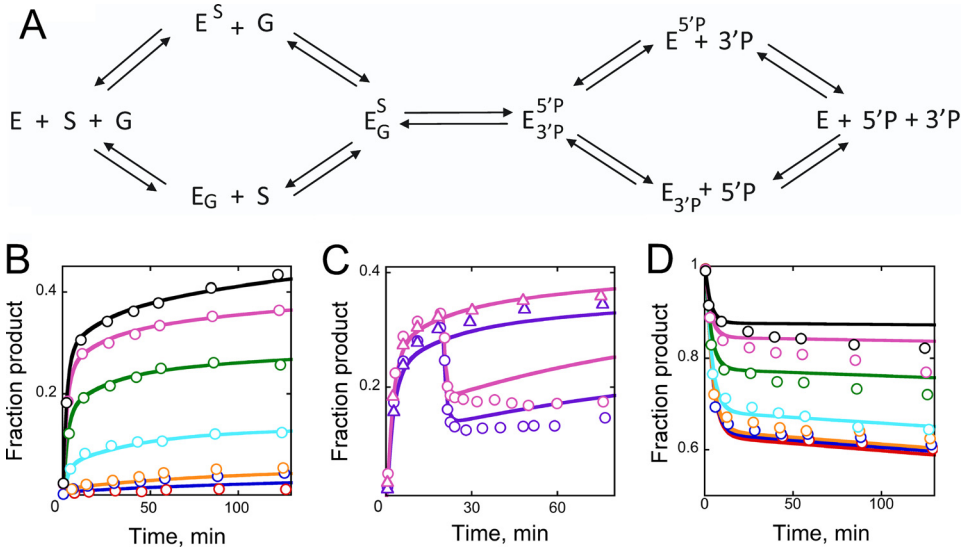

FIGURE 3. **Substrate cleavage and ligation by prefolded ribozyme.** *A*, schematic of reaction steps used in modeling results in subsequent panels. K_{INT} represents the internal equilibrium between substrate cleavage and ligation. *E*, *Azoarcus* ribozyme; *G*, guanosine; *S*, ribozyme substrate CAUACGGCC; *5′P*, reaction product CAU; *3′P*, reaction product GACGGCC; *S*, substrate CAUACGGCC. *B*, varying guanosine concentration in substrate cleavage reactions at 25 °C, 50 mM Mg^{2+} after prefolding the ribozyme as above. Guanosine was absent (*red*) or present at 1 μM (*blue*), 2 μM (*orange*), 10 μM (*cyan*), 50 μM (*green*), 200 μM (*pink*), or 1000 μM (*black*). *C*, dilution of guanosine (10-fold, *circles*) after allowing formation of internal equilibrium for substrate cleavage reactions. Initial guanosine concentrations are 100 μM (*purple*) or 200 μM (*pink*). Also shown are results from parallel reactions in which the guanosine concentration was held constant during the 10-fold dilution (*triangles*). *D*, ligation reactions starting from products (25 °C, 50 mM Mg^{2+}). Guanosine concentrations are shown using the same colors as in *B*. The curves in *B–D* reflect global fits using Kinetic Explorer (Ref. 62; see supplemental Table S1 for rate and equilibrium constants) (Refs. 63 and 64). Reactions equivalent to those in *B* and *D* but performed at lower Mg^{2+} concentration (10 mM) are shown in supplemental Fig. S2. Reactions analogous to those in *B* and supplemental Fig. S2*A* but with the substrate prebound to the ribozyme are shown in supplemental Fig. S1.

indicating that the ribozyme was fully bound to the substrate. The substoichiometric product formation could indicate that a fraction of the ribozyme was inactive, because it was either damaged or misfolded. Alternatively or in addition, it was possible that the cleavage products were religated faster than they were released from the ribozyme. This behavior would give reformation of substrate and guanosine and formation of an internal equilibrium between substrate and products (K_{INT} in Fig. 3*A*) (43, 44), reminiscent of the self-splicing reaction by the intact intron (34). In this case, the amount of product could be substantially less than the amount of active ribozyme. To determine the amount of native ribozyme from the amount of product produced, it would be necessary to determine this internal equilibrium value.

Therefore, we first varied the guanosine concentration in cleavage reactions with the idea that, if substrate cleavage and ligation reach equilibrium and guanosine binding is readily reversible, lower guanosine concentrations will result in smaller product bursts because incomplete guanosine binding will shift the equilibrium toward the substrate (Fig. 3*A*). Indeed, we found a strong dependence of the burst amplitude on guanosine concentration (Fig. 3*B*). There was little or no effect on the rate constant, as expected for rate-limiting substrate binding. We tested this model further by generating a large burst by using high guanosine concentration and then diluting the reaction to a lower guanosine concentration. As predicted from this model, upon dilution we observed a re-equilibration with rapid formation of the substrate and loss of the product (Fig. 3*C*).

Finally, to provide additional constraints for global modeling of the cleavage and ligation reactions and determination of the value of the internal equilibrium, we performed a series of reactions analogous to those in Fig. 3*B* but starting from the products (0.8 μM of each product, 2-fold in excess of ribozyme). These reactions gave bursts of substrate formation, and as expected, the bursts were smaller with high guanosine concentrations and largest in the absence of added guanosine (Fig. 3*D*). Analogous reactions at 10 mM Mg^{2+} are shown in supplemental Fig. S2.

All of the results in Fig. 3 and supplemental Fig. S2 were fit using global models, with one set of rate and equilibrium constants for reactions at 50 mM Mg^{2+} and a second set for reactions at 10 mM Mg^{2+} (supplemental Table S1). The value of the internal equilibrium is approximately unity at 10 mM Mg^{2+} (1.2) and rises to 2.1 at 50 mM Mg^{2+}, accounting for the larger bursts of product formation at 50 mM Mg^{2+} (Fig. 2). To calculate the amount of native ribozyme from the amount of product produced, it is necessary to account for the ribozyme that is active but remains substrate-bound as this internal equilibrium is reached. Multiplying the burst amplitudes for prefolded ribozyme with saturating guanosine concentration (Fig. 3*B* and supplemental Fig. S2*A*) by the correction factor $((K_{int} + 1)/K_{int})$ gives calculated values of active ribozyme that are the same within error as the total amount of ribozyme.

Together, the results above indicate that the ribozyme folds to completion in less than 15 min at 37 °C and that most or all of the ribozyme is present in the native state at equilibrium under these conditions. This result indicates that the native conformation is more stable than any accessible misfolded conformations. In the sections below, we use the information on the catalytic reaction and equilibrium folding to measure the kinetics of native ribozyme folding.

Monitoring Ribozyme Folding by Catalytic Activity—To measure the time dependence of native ribozyme formation

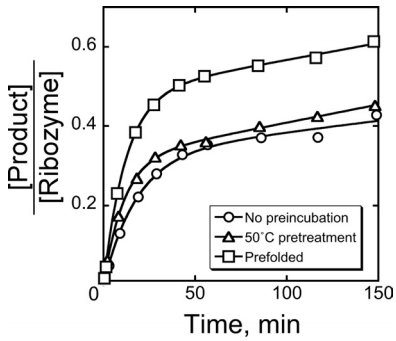

FIGURE 4. **Continuous folding and catalytic activity assay.** The folding and catalytic reactions were initiated simultaneously by adding the ribozyme (0.4 μM) to 10 mM Mg^{2+} and 0.8 μM substrate at 25 °C (*circles*). Also shown is a reaction in which the ribozyme was preincubated for 10 min at 50 °C in the absence of Mg^{2+} before Mg^{2+} and substrate were added together (*triangles*) and a reaction in which the ribozyme was prefolded for 30 min at 37 °C in 10 mM Mg^{2+} and then the substrate was added (*squares*). The burst amplitude of this prefolded ribozyme reaction corresponded to 24% of the input substrate (48% of the ribozyme with 2-fold substrate excess). After corrections for the internal equilibrium for cleavage and ligation (K_{eq} = 1.2 under these conditions; see supplemental Table S1) and the subsaturating guanosine concentration (100 μM; K_D = 110–120 μM; see supplemental Table S1), this burst amplitude corresponds to a homogeneous population of native ribozyme.

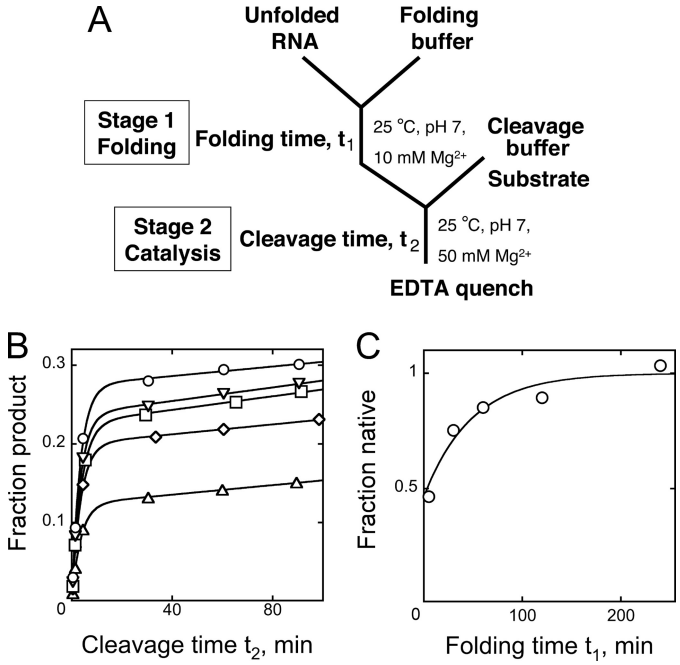

FIGURE 5. **Slow accumulation of native ribozyme.** *A*, schematic of the discontinuous assay for *Azoarcus* ribozyme folding. The ribozyme folds in stage 1, and portions of the reaction are transferred to stage 2 to measure the fraction of native ribozyme. *B*, the ribozyme was folded in stage 1 (25 °C, 10 mM Mg^{2+}) for 5 min (*triangles*), 30 min (*diamonds*), 60 min (*squares*), 120 min (*inverted triangles*), or 240 min (*circles*) before being transferred to stage 2 (50 mM Mg^{2+}). The larger bursts with increased folding time (t_1) indicate accumulation of the native ribozyme on this time scale. *C*, burst amplitude from reactions in *B* plotted against folding time, t_1, at 25 °C and 10 mM Mg^{2+}. The *y* axis values are normalized by the apparent end point, which corresponded to 53 ± 4% of the substrate, nearly the same as obtained by prefolding the ribozyme at 37 °C.

using catalytic activity, we first performed experiments analogous to those above but without a folding preincubation. Thus, we added substrate simultaneously with Mg^{2+}, so that ribozyme folding and substrate cleavage would occur in the same reaction (termed a continuous assay; Ref. 18). If the entire ribozyme population folded to the native state with at least as large a rate constant as the substrate is cleaved by the folded ribozyme, the progress of substrate cleavage would be identical with or without a folding preincubation. On the other hand, if some of the ribozyme did not reach the native state rapidly, less substrate would be cleaved rapidly in the reaction without the prefolding step.

When Mg^{2+} and substrate were added simultaneously to the ribozyme at 25 °C, a burst of product was formed with a rate constant of ~0.1 min^{-1}, the expected rate constant for binding-limited substrate cleavage. Thus, a fraction of the ribozyme folded rapidly to the native state (Fig. 4). However, a parallel reaction in which the ribozyme was prefolded in 10 mM Mg^{2+} (37 °C, 10 min) displayed a larger burst, in the range observed previously with the same guanosine concentration (Fig. 2*A*). The amplitude from the folding reaction was 65% that of the prefolded control, indicating that approximately two-thirds of the ribozyme folded to the native state with a rate constant larger than that for substrate binding and cleavage, whereas the remaining third did not reach the native state on the time scale of substrate cleavage. Pretreatment of the unfolded ribozyme by incubating it at 50 °C for 10 min (39) gave a small but detectable increase in the fraction of ribozyme that folded rapidly to the native state upon addition of Mg^{2+} and substrate (Fig. 4), suggesting that the initial conformation of the ribozyme influences the folding outcome for this small subpopulation (13, 15, 45) but that the slow folding pathway remains extensively populated.

To explore the slow folding further, we used a discontinuous assay (18), in which portions of a folding reaction (termed stage 1) are transferred at various times to stage 2, where the conditions allow rapid substrate cleavage, while minimizing further native folding (18). In stage 2 (25 °C, 50 mM Mg^{2+}), the substrate is added, and the fraction of the substrate that is cleaved rapidly provides a measure of the fraction of the ribozyme that was native at the time of the transfer (Fig. 5*A*). When folding (stage 1) was performed under the same conditions as the experiment in Fig. 4 (25 °C, 10 mM Mg^{2+}), the shortest accessible folding times gave bursts that corresponded to ~50% native ribozyme (Fig. 5, *B* and *C*). This value is similar but slightly lower than indicated by the continuous assay, suggesting that substrate binding during folding may give a small bias for native folding. As folding time was increased, the burst amplitude increased slowly (k = 0.02 min^{-1}), ultimately approaching the level of prefolded ribozyme and indicating 90–100% native ribozyme. We also explored whether the fraction of ribozyme that folds slowly is affected by conditions of the folding reaction. When folding was performed at 15 or 37 °C, the same fraction was observed to reach the native state rapidly as at 25 °C. Further, when these reactions were transferred to 25 °C after a 5-min incubation, they gave the same rate constant for the slow accumulation of native ribozyme (0.02 min^{-1}), indicating that the same intermediate is formed at all three temperatures (data not shown).

Together, these experiments indicate that although much of the ribozyme folds to the native state in a few minutes or less, a substantial fraction populates one or more long-lived intermediates before ultimately reaching the thermodynamically

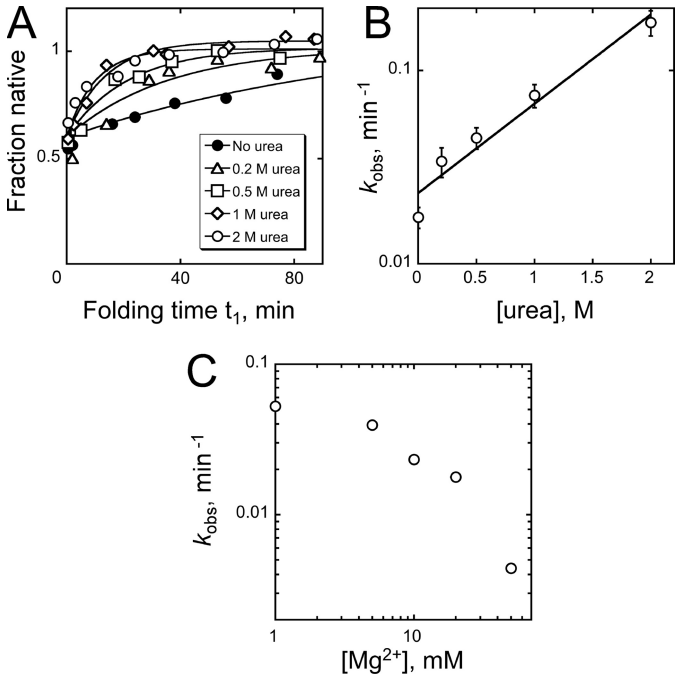

FIGURE 6. **Effects of urea and Mg^{2+} on refolding of the misfolded ribozyme.** *A*, refolding progress in the presence of urea. The misfolded ribozyme was first formed by incubating the ribozyme in the absence of urea (25 °C, 10 mM Mg^{2+}, 5 min), and then the ribozyme (8 μM) was transferred to a solution that included the desired urea concentration. At various times, portions of the reaction were withdrawn and diluted 20-fold into stage 2 to determine the fraction of native ribozyme. This dilution was much larger than for standard reactions to eliminate possible effects of urea on the cleavage reaction. The *y* axis values are normalized by the end point in the absence of urea, which corresponded to complete formation of the native ribozyme. *B*, dependence of refolding rate on urea concentration. The slope of the log-linear dependence gave a urea *m* value of 0.7 ± 0.1 kcal mol^{-1} M^{-1}. *C*, dependence of refolding rate on Mg^{2+} concentration. As in *A*, the misfolded ribozyme was first formed by incubating the ribozyme for 5 min under standard folding conditions, and then the ribozyme was transferred to solutions containing different Mg^{2+} concentrations for refolding.

favored native state with a half-life of ~30 min under these conditions. The simple first order transition to the native state most simply suggests that the slow folding results from formation of a single intermediate or an ensemble of rapidly converting intermediates, and work below provides further support for this conclusion.

A Kinetically Trapped Intermediate—To explore further the long-lived intermediate and its folding transition to the native state, we measured how changes in solution conditions affect the rate of the slow folding transition (17, 19, 46). The long-lived intermediate was formed by a short incubation under constant conditions (5 min at 25 °C, 10 mM Mg^{2+}), and then conditions were changed for stage 1 by adding urea or by varying Mg^{2+} concentration or temperature, and at various times aliquots were trapped in stage 2 (25 °C, 50 mM Mg^{2+}). The fraction of native ribozyme was determined by catalytic activity as above. We found that the denaturant urea strongly accelerated the folding transition to the native state, giving an *m* value of −0.7 ± 0.1 kcal mol^{-1} M^{-1} and indicating that transient unfolding of the long-lived intermediate is required (Fig. 6, *A* and *B*). Increased Mg^{2+} concentration slowed the transition, suggesting that the intermediate is structured and stabilized by Mg^{2+} (Fig. 6*C*). Higher temperatures increased the rate, with an apparent activation enthalpy of 41 kcal/mol (supplemental Fig. S3, *A* and *B*). Together, these results indicate that the intermediate is misfolded and must be at least partially unfolded to allow refolding to the native state.

We also measured folding under conditions used in recent SAXS experiments (39). This prior work revealed a small but detectable phase of compaction, which occurred on the minutes time scale and presumably reflected slow native folding of a fraction of the ribozyme population. Although the small magnitude of the change was interpreted to indicate participation of only a small fraction of the ribozyme, we found that half of the population formed the intermediate, the same within error as under our standard conditions (supplemental Fig. S3*C*). Refolding to the native state gave a rate constant of 0.29 min^{-1}, the same within error as that detected by SAXS. Thus, the two approaches likely monitor the same folding transition, and the small change observed by SAXS most likely reflects that the misfolded intermediate is compact and resembles the fully folded structure.

Together these results indicate that, under a wide range of conditions, approximately half of the ribozyme misfolds to an intermediate that refolds slowly to the native state in a process that requires transient unfolding. Misfolding was demonstrated previously for the pre-tRNA containing this intron, but its refolding is accelerated much less by urea and is accelerated, not slowed, by increased Mg^{2+} concentration (46). Thus, the pre-tRNA most likely forms a different misfolded conformation, at least under the conditions of this previous work, consistent with the authors' interpretation of non-native interactions with exon sequences. On the other hand, our results are reminiscent of misfolding by the *Tetrahymena* group I intron ribozyme (17, 47), raising the possibility of common features in the folding and misfolding of these two RNAs (see "Misfolding of the Azoarcus Ribozyme" under "Discussion").

Acceleration of Refolding by DEAD Box Proteins—We also investigated the effects of the DEAD box proteins CYT-19 and Mss116p on *Azoarcus* ribozyme refolding. Using the discontinuous assay, we first folded the ribozyme to a mixture of the native and misfolded conformations and then added CYT-19 or Mss116p in the presence or absence of ATP. At various times, further folding was blocked by increasing Mg^{2+} concentration to 50 mM, and the fraction of native ribozyme was determined by catalytic activity as above. At relatively low concentrations of protein, just slightly in excess of the ribozyme, both DEAD box proteins accelerated the formation of native ribozyme (Fig. 7). These accelerations required ATP, because omitting nucleotide or including the nonhydrolyzable analog AMP-PNP (2 mM) gave no detectable acceleration and decreased the end point somewhat, perhaps by trapping folding intermediates (Fig. 7, *A* and *C*, and data not shown). The efficiency of the reaction was moderately larger for Mss116p than for CYT-19, qualitatively consistent with previous work in which splicing was monitored for several different group I and group II introns (24, 27). At higher protein concentrations, the folding rates reached a plateau and possibly decreased for Mss116p, most likely reflecting stable binding to RNA folding intermediates and/or ATP-dependent disruption of the native state (24, 33).

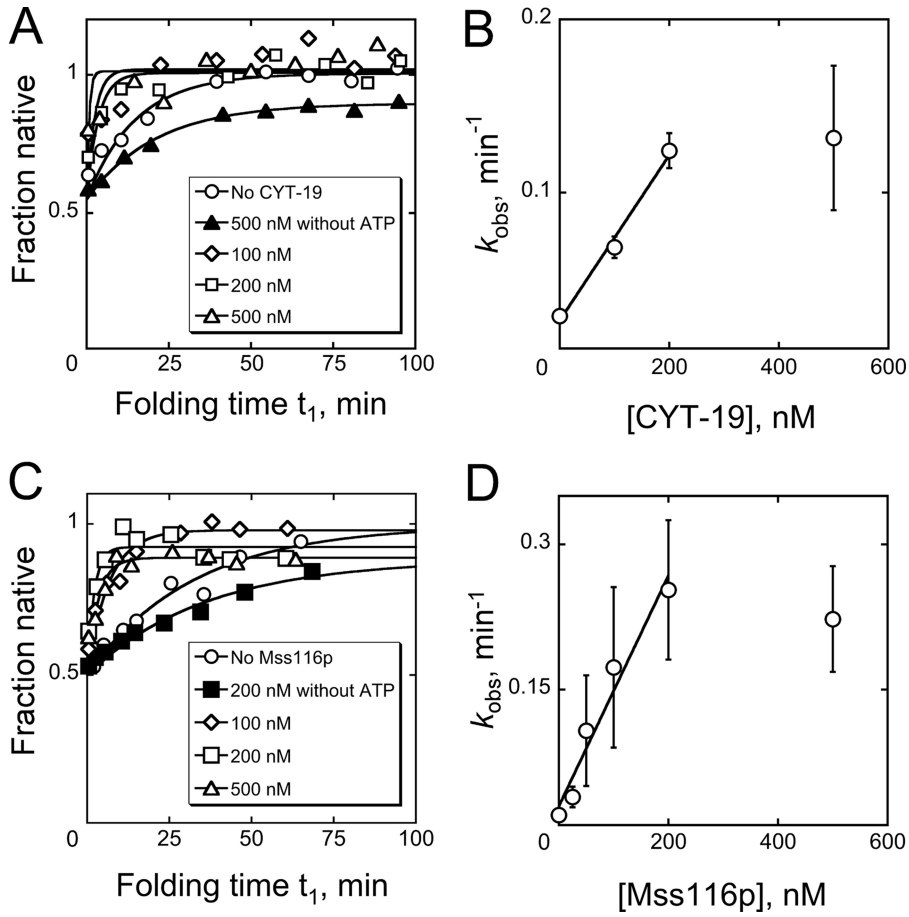

FIGURE 7. **Acceleration of ribozyme refolding by DEAD box proteins CYT-19 and Mss116p.** *A* and *B*, progress curves and protein concentration dependence for ribozyme refolding in the presence of CYT-19. *C* and *D*, progress curves and concentration dependence for refolding with Mss116p. The dependences of observed rate constant on CYT-19 and Mss116p concentrations gave second order rate constants of 4.8 (± 0.5) × 10^5 M^{-1} min^{-1} and 1.2 (± 0.2) × 10^6 M^{-1} min^{-1}, respectively, from linear fits within the concentration regimes that gave folding activation. The apparent breakpoints at higher protein concentrations presumably reflect the intersection of activation and inhibition, as observed for other ribozymes (24, 33). In *A* and *C*, the *y* axis values are normalized by the endpoints in the absence of protein. The reactions included 2 mM ATP-Mg^{2+} unless otherwise indicated.

DISCUSSION

Here, we designed and used assays to monitor native folding of the *Azoarcus* group I intron ribozyme by measuring the onset of its catalytic activity. We found that a substantial fraction of the ribozyme population folds to a long-lived intermediate that displays experimental hallmarks of a misfolded conformer and is accelerated for refolding by the DEAD box chaperone proteins Mss116p and CYT-19. These results have important parallels to previous findings for other group I introns and highlight the pervasive nature of RNA misfolding and RNA chaperone activity (15, 17, 48–50).

Catalytic Activity as a Probe of Azoarcus Ribozyme Folding—Catalytic activity provides a powerful probe that is complementary to physical approaches because it can readily distinguish the native state from all inactive conformations, regardless of how similar they are structurally. For the *Azoarcus* ribozyme, catalytic activity has been used previously to measure the Mg^{2+} dependence of equilibrium folding and cleavage (51), and it has recently been used to measure the relative folding progress, providing quantitative information on folding rates and relative measures of the extent of native folding (40).

By delineating the properties of the substrate cleavage and ligation reactions, our results allow the amplitudes of product formation, as well as the rate constants, to be interpreted quantitatively. Slow release of both products leads to the formation of an internal equilibrium between cleavage and ligation, such that the amount of product formed rapidly is less than the amount of native ribozyme. This conclusion is qualitatively consistent with previous work in which the maximal cleavage burst reflected 40% of the substrate in single turnover reactions (51).

With regard to the slow release of products, it is striking that the 5′ product (CAU) is released in tens of minutes because it would be expected to dissociate from base pairs with its partner strand, the internal guide sequence of the ribozyme, in milliseconds (52, 53). Slow dissociation is also supported by pulse-chase experiments, which gave a rate constant of 0.1 min^{-1} at 50 °C[5] and previous work that established a K_m value of 50 nM (54). Tight binding presumably stems from strong tertiary interactions between the product-containing duplex and the ribozyme body. These contacts are inherent to group I introns and position the reactive groups in the active site, but their strength can vary widely (55–57). It is notable that substrate binding is also quite slow (<10^6 M^{-1} min^{-1}), ~100-fold slower than binding

[5] X. Yuan and R. Russell, unpublished results.

of the *Tetrahymena* ribozyme to its substrate and 1000-fold slower than simple duplex formation (44, 58). It is possible that the internal guide sequence of the *Azoarcus* ribozyme is sequestered by interactions with the ribozyme body in the absence of its partner strand.

Misfolding of the Azoarcus Ribozyme—Early work suggested that this ribozyme avoided long-lived intermediates and folded to the native state in milliseconds, but more recent experiments have demonstrated the presence of intermediates and slower folding steps for at least a fraction of the population (39, 40). By tracking formation of the native state directly, our results build on these findings by showing that it is a large fraction, approximately half of the ribozyme, that reaches the native state slowly, on the time scale of an hour under our conditions. Our results are consistent with a recent study in which footprinting and kinetic modeling suggested two dominant pathways, populated approximately equally, which give fully folded ribozyme with rate constants of ~2 and 0.2 min^{-1} at 37 °C (40). This study provided rate information on the faster process, which was not probed in our work beyond giving a lower limit of ~0.1 min^{-1} (Fig. 4), and it gave a rate constant for the slower phase that is consistent with our measurements at 37 °C (supplemental Fig. S3). Our results demonstrate that both of these pathways result in native state formation and that all or nearly all of the ribozyme is present in the native state at the completion of these two folding phases, indicating that the native state is substantially more stable in solution than accessible alternative conformations.

Our results also give new insights into the nature of the slow folding pathway. The rate-limiting folding transition is accelerated by urea and increased temperature and decreased by increasing Mg^{2+} concentration, indicating that it involves a transient loss of structure and therefore reflects refolding of one or more misfolded intermediates. Under all of the conditions tested, we observed single exponential kinetics for native state formation, most simply suggesting that a single intermediate or ensemble of interconverting intermediates limits folding to the native state. This misfolded intermediate is probably highly structured, because the urea dependence for its transition to the native state corresponds to the transient exposure of ~10 base pairs (59). This interpretation is also supported by prior work indicating only small differences between the native state and the intermediate as monitored by hydroxyl radical footprinting (36, 37, 40) or by SAXS (39). These prior results also suggest that the intermediate bears a strong resemblance to the native state and most likely includes substantial native structure. The ribozyme is stabilized by two canonical tetraloop-receptor interactions (34, 35) (Fig. 1) and forms native tertiary contacts cooperatively (37, 51, 60). Some of these tertiary contacts may be able to form and stabilize the misfolded structure.

The properties of the misfolded conformation and its transition to the native state resemble those of the *Tetrahymena* ribozyme, which also partitions between pathways in folding, giving predominantly a misfolded conformation that includes extensive native structure, refolds slowly, and gives qualitatively similar dependences on temperature and Mg^{2+} and urea concentrations. This misfolded conformation involves structural differences in the core, which are suggested to originate from an altered topology (17, 19). The *Tetrahymena* ribozyme is larger than the *Azoarcus* ribozyme and has more peripheral structure, but both RNAs have the same core elements and native state topology. It is possible that the misfolded conformations of these ribozymes are structurally related, with the more extensive peripheral structure and contacts of the *Tetrahymena* ribozyme stabilizing the misfolded conformation so that it is longer-lived and gives a greater urea dependence (1.7 kcal mol^{-1} M^{-1} (17), compared with 0.7 kcal mol^{-1} M^{-1} for the *Azoarcus* ribozyme; Fig. 6*B*). Nevertheless, there may be many folding intermediates with these properties, and further work will be necessary to address whether the misfolded forms of the two introns have related structures and physical origins.

Accelerated Refolding by DEAD Box Proteins—In keeping with their physiological roles as general RNA chaperone proteins (8, 9), both CYT-19 and Mss116p accelerate refolding of the misfolded *Azoarcus* ribozyme to the native state. For both proteins, detectable acceleration requires ATP, suggesting that the acceleration involves ATP-dependent disruption of structure within the misfolded intermediate. This disruption may include unwinding of ribozyme helices, because both proteins have been shown to use ATP to unwind short helices efficiently (20, 24, 27, 42, 61). Because the misfolded ribozyme appears to be compact and extensively structured, it is likely that tertiary contacts must also be disrupted, either directly or indirectly, and the required unfolding may include native structure as well as non-native structure. The observed net conversion of misfolded to native structure presumably arises because of the greater stability of the native structure (21), as indicated by its accumulation at equilibrium in the absence of protein. We expect that this folding transition of the *Azoarcus* ribozyme will be useful for further probing of the origins of RNA misfolding and the mechanisms of DEAD box proteins in RNA folding.

Acknowledgments—We thank Matthew Kanke for performing early experiments on ribozyme refolding by CYT-19, Ken Johnson for the Kinetic Explorer simulation program, and Inga Jarmoskaite and other members of the Russell lab for helpful comments on the manuscript.

REFERENCES

1. Treiber, D. K., and Williamson, J. R. (1999) *Curr. Opin. Struct. Biol.* **9,** 339–345
2. Shcherbakova, I., Mitra, S., Laederach, A., and Brenowitz, M. (2008) *Curr. Opin. Chem. Biol.* **12,** 655–666
3. Russell, R. (2008) *Front Biosci.* **13,** 1–20
4. Fairman-Williams, M. E., Guenther, U. P., and Jankowsky, E. (2010) *Curr. Opin. Struct. Biol.* **20,** 313–324
5. Pan, C., and Russell, R. (2010) *RNA Biol.* **7,** 667–676
6. Jankowsky, E. (2011) *Trends Biochem. Sci.* **36,** 19–29
7. Jarmoskaite, I., and Russell, R. (2011) *WIREs RNA* **2,** 135–152
8. Mohr, S., Stryker, J. M., and Lambowitz, A. M. (2002) *Cell* **109,** 769–779
9. Huang, H. R., Rowe, C. E., Mohr, S., Jiang, Y., Lambowitz, A. M., and Perlman, P. S. (2005) *Proc. Natl. Acad. Sci. U.S.A.* **102,** 163–168
10. Woodson, S. A. (2010) *Annu. Rev. Biophys.* **39,** 61–77
11. Sclavi, B., Sullivan, M., Chance, M. R., Brenowitz, M., and Woodson, S. A. (1998) *Science* **279,** 1940–1943
12. Russell, R., Millett, I. S., Doniach, S., and Herschlag, D. (2000) *Nat. Struct. Biol.* **7,** 367–370

13. Russell, R., Zhuang, X., Babcock, H. P., Millett, I. S., Doniach, S., Chu, S., and Herschlag, D. (2002) *Proc. Natl. Acad. Sci. U.S.A.* **99,** 155–160
14. Kwok, L. W., Shcherbakova, I., Lamb, J. S., Park, H. Y., Andresen, K., Smith, H., Brenowitz, M., and Pollack, L. (2006) *J. Mol. Biol.* **355,** 282–293
15. Laederach, A., Shcherbakova, I., Jonikas, M. A., Altman, R. B., and Brenowitz, M. (2007) *Proc. Natl. Acad. Sci. U.S.A.* **104,** 7045–7050
16. Russell, R., and Herschlag, D. (1999) *J. Mol. Biol.* **291,** 1155–1167
17. Russell, R., Das, R., Suh, H., Travers, K. J., Laederach, A., Engelhardt, M. A., and Herschlag, D. (2006) *J. Mol. Biol.* **363,** 531–544
18. Wan, Y., Mitchell, D., 3rd, and Russell, R. (2009) *Methods Enzymol.* **468,** 195–218
19. Wan, Y., Suh, H., Russell, R., and Herschlag, D. (2010) *J. Mol. Biol.* **400,** 1067–1077
20. Tijerina, P., Bhaskaran, H., and Russell, R. (2006) *Proc. Natl. Acad. Sci. U.S.A.* **103,** 16698–16703
21. Bhaskaran, H., and Russell, R. (2007) *Nature* **449,** 1014–1018
22. Johnson, T. H., Tijerina, P., Chadee, A. B., Herschlag, D., and Russell, R. (2005) *Proc. Natl. Acad. Sci. U.S.A.* **102,** 10176–10181
23. Del Campo, M., Tijerina, P., Bhaskaran, H., Mohr, S., Yang, Q., Jankowsky, E., Russell, R., and Lambowitz, A. M. (2007) *Mol. Cell* **28,** 159–166
24. Del Campo, M., Mohr, S., Jiang, Y., Jia, H., Jankowsky, E., and Lambowitz, A. M. (2009) *J. Mol. Biol.* **389,** 674–693
25. Solem, A., Zingler, N., and Pyle, A. M. (2006) *Mol. Cell* **24,** 611–617
26. Mohr, S., Matsuura, M., Perlman, P. S., and Lambowitz, A. M. (2006) *Proc. Natl. Acad. Sci. U.S.A.* **103,** 3569–3574
27. Halls, C., Mohr, S., Del Campo, M., Yang, Q., Jankowsky, E., and Lambowitz, A. M. (2007) *J. Mol. Biol.* **365,** 835–855
28. Bifano, A. L., and Caprara, M. G. (2008) *J. Mol. Biol.* **383,** 667–682
29. Fedorova, O., Solem, A., and Pyle, A. M. (2010) *J. Mol. Biol.* **397,** 799–813
30. Bifano, A. L., Turk, E. M., and Caprara, M. G. (2010) *J. Mol. Biol.* **398,** 429–443
31. Zingler, N., Solem, A., and Pyle, A. M. (2010) *Nucleic Acids Res.* **38,** 6602–6609
32. Karunatilaka, K. S., Solem, A., Pyle, A. M., and Rueda, D. (2010) *Nature* **467,** 935–939
33. Potratz, J. P., Del Campo, M., Wolf, R. Z., Lambowitz, A. M., and Russell, R. (2011) *J. Mol. Biol.* **411,** 661–679
34. Tanner, M., and Cech, T. (1996) *RNA* **2,** 74–83
35. Adams, P. L., Stahley, M. R., Kosek, A. B., Wang, J., and Strobel, S. A. (2004) *Nature* **430,** 45–50
36. Rangan, P., Masquida, B., Westhof, E., and Woodson, S. A. (2003) *Proc. Natl. Acad. Sci. U.S.A.* **100,** 1574–1579
37. Chauhan, S., and Woodson, S. A. (2008) *J. Am. Chem. Soc.* **130,** 1296–1303
38. Chauhan, S., Behrouzi, R., Rangan, P., and Woodson, S. A. (2009) *J. Mol. Biol.* **386,** 1167–1178
39. Roh, J. H., Guo, L., Kilburn, J. D., Briber, R. M., Irving, T., and Woodson, S. A. (2010) *J. Am. Chem. Soc.* **132,** 10148–10154
40. Mitra, S., Laederach, A., Golden, B. L., Altman, R. B., and Brenowitz, M. (2011) *RNA* **17,** 1589–1603
41. Zaug, A. J., Grosshans, C. A., and Cech, T. R. (1988) *Biochemistry* **27,** 8924–8931
42. Grohman, J. K., Del Campo, M., Bhaskaran, H., Tijerina, P., Lambowitz, A. M., and Russell, R. (2007) *Biochemistry* **46,** 3013–3022
43. Golden, B. L., and Cech, T. R. (1996) *Biochemistry* **35,** 3754–3763
44. Karbstein, K., Carroll, K. S., and Herschlag, D. (2002) *Biochemistry* **41,** 11171–11183
45. Pan, J., Thirumalai, D., and Woodson, S. A. (1997) *J. Mol. Biol.* **273,** 7–13
46. Rangan, P., Masquida, B., Westhof, E., and Woodson, S. A. (2004) *J. Mol. Biol.* **339,** 41–51
47. Russell, R., and Herschlag, D. (2001) *J. Mol. Biol.* **308,** 839–851
48. Pan, J., and Woodson, S. A. (1998) *J. Mol. Biol.* **280,** 597–609
49. Zhang, L., Xiao, M., Lu, C., and Zhang, Y. (2005) *RNA* **11,** 59–69
50. Jiang, Y. F., Xiao, M., Yin, P., and Zhang, Y. (2006) *RNA* **12,** 561–566
51. Chauhan, S., Caliskan, G., Briber, R. M., Perez-Salas, U., Rangan, P., Thirumalai, D., and Woodson, S. A. (2005) *J. Mol. Biol.* **353,** 1199–1209
52. Freier, S. M., Kierzek, R., Jaeger, J. A., Sugimoto, N., Caruthers, M. H., Neilson, T., and Turner, D. H. (1986) *Proc. Natl. Acad. Sci. U.S.A.* **83,** 9373–9377
53. Serra, M. J., and Turner, D. H. (1995) *Methods Enzymol.* **259,** 242–261
54. Strauss-Soukup, J. K., and Strobel, S. A. (2000) *J. Mol. Biol.* **302,** 339–358
55. Narlikar, G. J., and Herschlag, D. (1996) *Nat. Struct. Biol.* **3,** 701–710
56. Testa, S. M., Haidaris, C. G., Gigliotti, F., and Turner, D. H. (1997) *Biochemistry* **36,** 15303–15314
57. Kuo, L. Y., Davidson, L. A., and Pico, S. (1999) *Biochim. Biophys. Acta* **1489,** 281–292
58. Herschlag, D., and Cech, T. R. (1990) *Biochemistry* **29,** 10159–10171
59. Shelton, V. M., Sosnick, T. R., and Pan, T. (1999) *Biochemistry* **38,** 16831–16839
60. Moghaddam, S., Caliskan, G., Chauhan, S., Hyeon, C., Briber, R. M., Thirumalai, D., and Woodson, S. A. (2009) *J. Mol. Biol.* **393,** 753–764
61. Yang, Q., Del Campo, M., Lambowitz, A. M., and Jankowsky, E. (2007) *Mol. Cell* **28,** 253–263
62. Johnson, K. A., Simpson, Z. B., and Blom, T. (2009) *Anal. Biochem.* **387,** 20–29
63. McConnell, T. S., Cech, T. R., and Herschlag, D. (1993) *Proc. Natl. Acad. Sci. U.S.A.* **90,** 8362–8366
64. Mei, R., and Herschlag, D. (1996) *Biochemistry* **35,** 5796–5809

The *Azoarcus* Group I Intron Ribozyme Misfolds and Is Accelerated for Refolding by ATP-dependent RNA Chaperone Proteins

Selma Sinan, Xiaoyan Yuan and Rick Russell

J. Biol. Chem. 2011, 286:37304-37312.
doi: 10.1074/jbc.M111.287706 originally published online August 30, 2011